Earth Planets Space, **64**, 743–752, 2012

Automated recognition of spikes in 1 Hz data recorded at the Easter Island magnetic observatory

Anatoly Soloviev[1], Arnaud Chulliat[2], Shamil Bogoutdinov[1], Alexei Gvishiani[1], Sergey Agayan[1], Aline Peltier[2], and Benoit Heumez[2]

[1]*Geophysical Center of the Russian Academy of Sciences (GC RAS), Russia*
[2]*Institut de Physique du Globe de Paris (IPGP), France*

(Received June 7, 2011; Revised February 24, 2012; Accepted March 22, 2012; Online published September 18, 2012)

In the present paper we apply a recently developed pattern recognition algorithm *SPs* to the problem of automated detection of artificial disturbances in one-second magnetic observatory data. The *SPs* algorithm relies on the theory of discrete mathematical analysis, which has been developed by some of the authors for more than 10 years. It continues the authors' research in the morphological analysis of time series using fuzzy logic techniques. We show that, after a learning phase, this algorithm is able to recognize artificial spikes uniformly with low probabilities of target miss and false alarm. In particular, a 94% spike recognition rate and a 6% false alarm rate were achieved as a result of the algorithm application to raw one-second data acquired at the Easter Island magnetic observatory. This capability is critical and opens the possibility to use the *SPs* algorithm in an operational environment.

Key words: Magnetic observatory, magnetogram, spikes, pattern recognition, fuzzy logic.

1. Introduction

The global network of magnetic observatories is one of the main observation infrastructures for geomagnetic research. Magnetic observatory data are used for investigating the geomagnetic secular variation originating in the Earth's outer core, as well as the rapid variations generated by electric currents in the ionosphere, the magnetosphere and the oceans (e.g., recent papers such as Love, 2008; Matzka *et al*., 2010). They are also used by a variety of governmental and industrial customers for applications such as directional drilling, reduction of magnetic survey data and space weather monitoring and forecasting (e.g., Reay *et al*., 2005; Marshall *et al*., 2011). Unlike other magnetometer networks, observatories are aimed at operating for several decades using internationally agreed standards of operations. About 120 observatories currently cooperate toward this goal within the INTERMAGNET program (www.intermagnet.org).

One of the main challenges faced by observatories is to being able to provide data of the highest quality on times scales ranging from one second to several decades. Up until a few years ago, most INTERMAGNET observatories were producing one-minute filtered data (from measurements sampled at a higher frequency, for example every 5 seconds; see St-Louis, 2008). However, in order to address the needs of the space physics community, several observatory programs have embarked into a modernization of their equipment in order to being able to produce one-second filtered data (e.g., Chulliat *et al*., 2009b; Worthington *et al*., 2009). As expected, the faster measurement sampling rate uncovered various signals that were previously filtered out in one-minute data, including some artificial disturbances that have to be removed from the final observatory data products. While at many observatories the one-second data cleaning represents a reasonable amount of work, it becomes a daunting task at some observatories, particularly those installed in remote but important locations where no optimal observatory site could be found. For example, it is the case at the recently installed magnetic observatory in Easter Island (Isla de Pascua Mataveri, IAGA code IPM; see Chulliat *et al*., 2009a and Fig. 1), where the close-by traffic of trucks and planes may generate more than hundred artificial disturbances every day.

In the present paper we apply a recently developed pattern recognition algorithm *SPs* (from SPIKEsecond) to the problem of automatically detecting artificial disturbances in one-second magnetic observatory data. The first important step towards automated magnetogram filtering was undertaken by Soloviev *et al*. (2009) and Bogoutdinov *et al*. (2010). The *SPs* algorithm relies on the theory of discrete mathematical analysis (Gvishiani *et al*., 2008a, 2010), which has been developed by some of the authors for more than 10 years. It continues the authors' research in the morphological analysis of time series using fuzzy logic techniques (see e.g., Agayan *et al*., 2005; Gvishiani *et al*., 2008a, b). We show that, after a learning phase, this algorithm is able to distinguish artificial disturbances from natural ones, such as short-period geomagnetic pulsations in the 1 s–1 min period range (e.g., Samson, 1991). This capability is critical and opens the possibility to use the *SPs* algorithm in an operational environment.

doi:10.5047/eps.2012.03.004

Fig. 1. Aerial view of the Isla de Pascua (Easter Island) magnetic observatory. The white, rectangular-shaped magnetometer container is located on the left side of the picture; the absolute hut is about 10 m to its right. Trucks circulating on the dirt road behind the observatory may generate more than hundred spikes per day.

2. Description of the *SPs* Algorithm

The *SPs* algorithm is a tool applicable to any time series that has specific time anomalies (disturbances), which have to be identified. The algorithm is aimed at recognition of singular spikes S of any nature with a simple morphology on a record y. (Note that *SPs* is not able to recognize jumps; this is done by another algorithm, JM, currently being developed by some of us.) An example of such spike, generated by a nearby running truck, is given in Fig. 2. The logic, which underlies the algorithm, is based on the following model of a spike. A **spike** S is defined as a record fragment having a **tip** $t(S)$, where two opposite **sharp slopes** S^l and S^r meet, surrounded by **quiet spike wings** $W^l(S)$ and $W^r(S)$ (Fig. 2). In order to formalize the logic of the algorithm, we use the concepts of fuzzy comparison and fuzzy extremality (Zadeh, 1965; Gvishiani *et al.*, 2008a, b). The detailed mathematical description of the algorithm is given in Soloviev *et al.* (2012). In what follows, we provide a brief summary of *SPs*.

The *SPs* algorithm consists of three blocks: "Λ-analysis", "Search for quasi-spikes" and "Selection of spikes" (Fig. 3). The starting record y is a time series $y = y(t)$ given on an interval of discrete positive semiaxis $\mathbb{R}_h^+ = \{t = kh,\ h > 0,\ k = 1, 2, \dots\}$, where h is the discretization step and k is the observation node.

The *SPs* algorithm begins its search by considering a local extremum of y as a possible tip $t = t(S)$ of a spike S. The algorithm evaluates the slopes S^l and S^r on each side of t. If they turn out to be sharp enough, the triplet $S = (S^l, t, S^r)$, referred to as a quasi-spike, is further examined. Next, the algorithm searches for quiet wings $W^l(S)$ and $W^r(S)$ to the left and to the right of S^l and S^r, respectively. If quiet wings are detected, the quasi-spike is recognized as a spike, as defined above. The algorithm is aimed specifically at recognizing such spikes on a record y.

The central part of the algorithm is the "Λ-analysis" (see Fig. 3), which provides a quantitative evaluation of the level of sharpness of slopes and the level of quietness of wings. It also distinguishes "ascending" and "descending" slopes. For a given fragment $\Delta^k y = \{y_k, \dots, y_{k+\Delta}\}$ of the record y, a linear regression (Draper and Smith, 1966) is calculated by the least-square technique. The regression coefficients are then used to determine whether the fragment is ascending or descending, and to derive an indicator of activity within the fragment. Determining whether this activity is large ("sharp" fragment) or small ("quiet" fragment) is performed by using fuzzy comparisons (Gvishiani *et al.*, 2008a, b) between a large number of fragments of varying lengths $\Lambda = \{\Delta_1, \dots, \Delta_m\}$. In *SPs*, the following fuzzy comparison function is used:

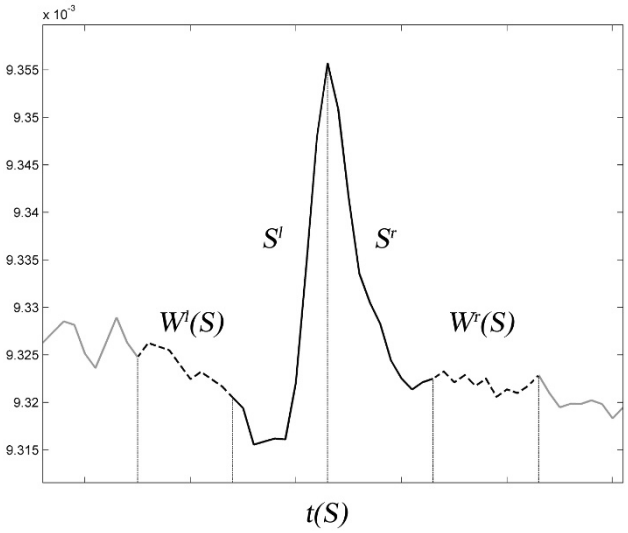

Fig. 2. Illustration of a spike S (solid black line) consisting of a tip $t(S)$ and two opposite sharp slopes S^l and S^r and surrounded by quiet left $W^l(S)$ and right $W^r(S)$ wings (dotted line).

$$n_\nu(A, B) = \frac{B - A}{(A^\nu + B^\nu)^{1/\nu}},$$
$$A \geq 0, \quad B \geq 0, \quad \nu > 0; \quad n_\nu(0, 0) = 0$$

for two numbers A and B, and where ν is a fixed parameter. It yields a number between -1 and 1 which quantifies how much B is larger than A.

The other blocks of *SPs* algorithm, "Search for quasi-spikes" and "Selection of spikes" (Fig. 3), use the de-

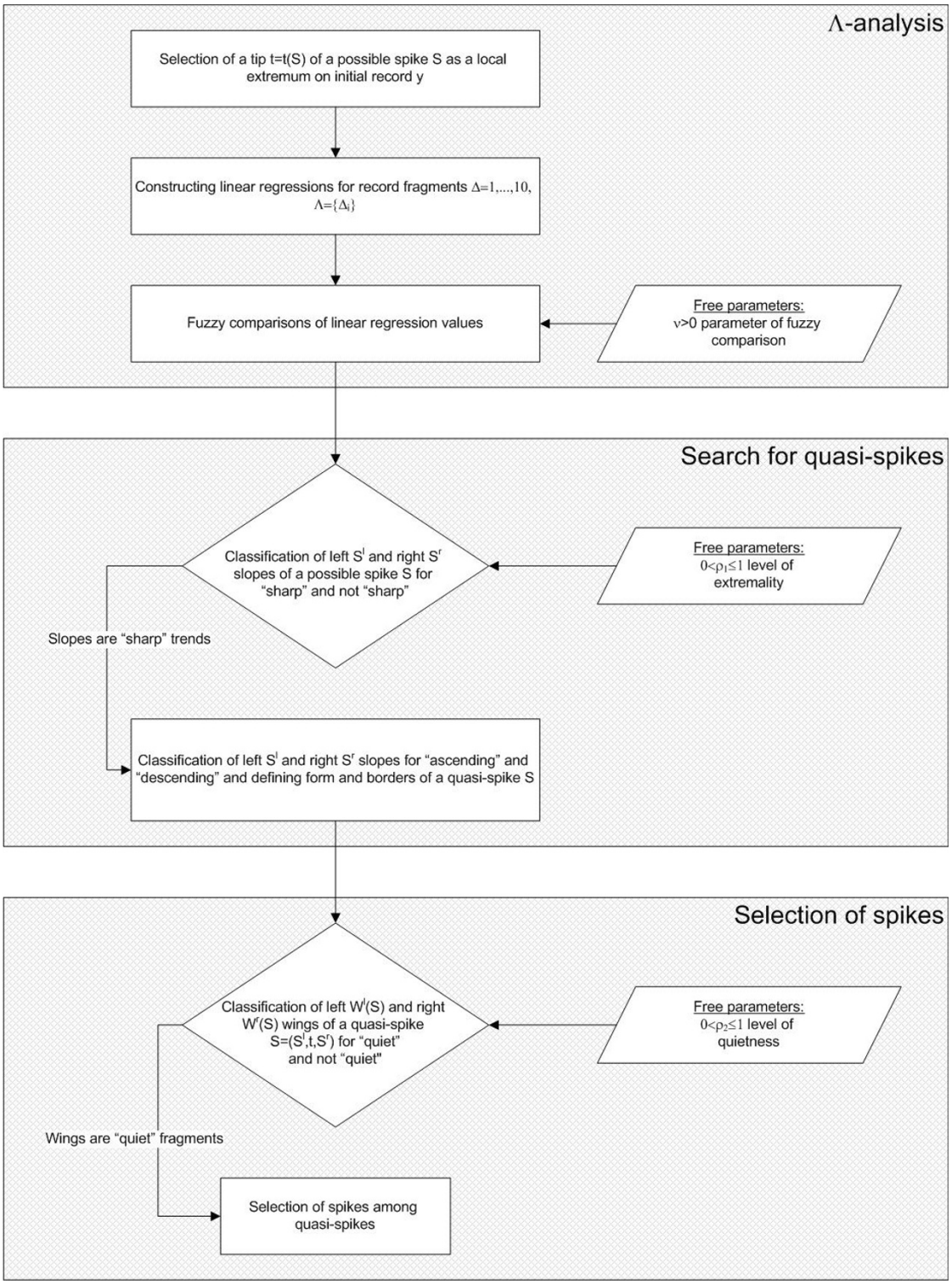

Fig. 3. Block scheme of the algorithm *SPs*.

scribed classifications and correspondingly identify quasi-spikes and choose genuine spikes among them.

The algorithm depends on the three free parameters $SPs = SPs\ (\nu, \rho_1, \rho_2)$ (Fig. 3):

ν—parameter of fuzzy comparison,

ρ_1—level of sharpness of the slopes S^l and S^r,

ρ_2—level of quietness of the wings $W^l(S)$ and $W^r(S)$.

A given set of free parameters is denoted by $\pi = (\nu, \rho_1, \rho_2)$.

3. Testing Dataset and Methodology

We tested the *SPs* algorithm on raw one-second data acquired at the Easter Island magnetic observatory in July and August 2009 (IPM, Fig. 1). The data include measurement values of the three components of the geomagnetic field vector along the North (X), East (Y) and downward vertical (Z) directions before baseline correction, and total intensity F of the geomagnetic field. Each 1-day 1-channel record registered with 1 Hz frequency consists of 86,400

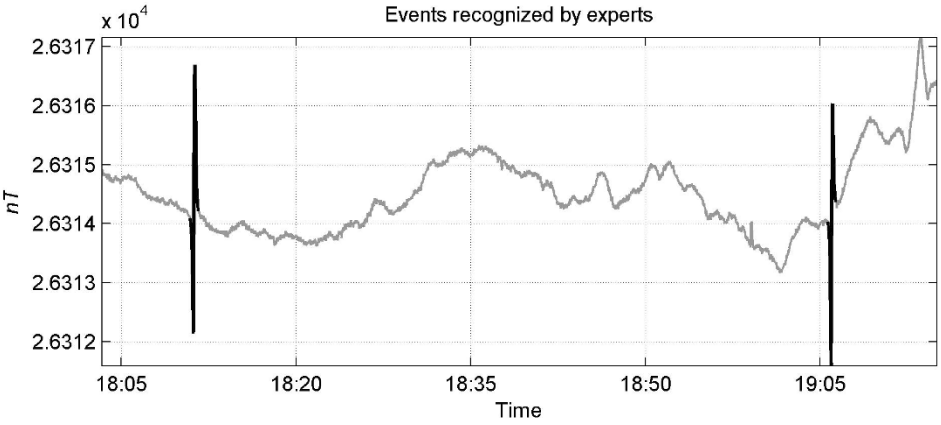

Fig. 4. Examples of artificial spikes removed after manual recognition (X component, 5 July 2009). Recognized spikes are marked with black.

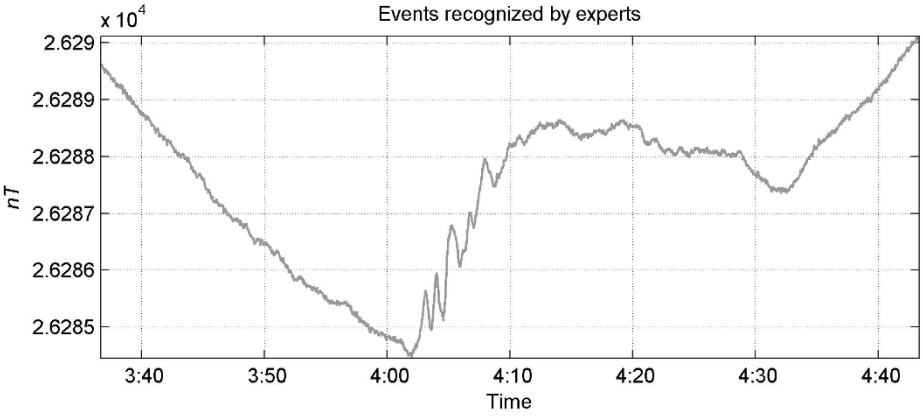

Fig. 5. Example of geomagnetic pulsations (X component, 1 July 2009).

Table 1. Statistical information on spikes from 01/07/2009 to 20/07/2009 recognized by eye on magnetograms.

Channel	Number of spikes	Min amplitude, nT	Max amplitude, nT	Mean amplitude, nT	Min duration, s	Max duration, s	Mean duration, s
X	1119	0.100	82.280	1.298	9	190	27.330
Y	1122	0.080	100.340	1.093	4	190	27.193
Z	996	0.100	20.640	0.371	6	470	28.861
F	1135	0.102	61.770	0.918	9	439	31.719

Table 2. Statistical information on spikes from 21/07/2009 to 31/07/2009 recognized by eye on magnetograms.

Channel	Number of spikes	Min amplitude, nT	Max amplitude, nT	Mean amplitude, nT	Min duration, s	Max duration, s	Mean duration, s
X	853	0.100	12.630	1.200	7	449	26.917
Y	844	0.140	12.430	0.972	9	449	27.096
Z	774	0.090	106.510	0.570	7	449	27.722
F	846	0.088	61.130	0.932	6	449	31.072

data points.

The testing dataset was entirely cleaned using standard observatory tools; i.e., spikes caused by trucks, planes and other artificial sources were manually removed after a detailed inspection of daily magnetograms. Figure 4 shows examples of such spikes. They have a characteristic shape, which makes them easily recognizable by eye. However, due to a vast amount of spikes in one-second magnetograms (around 2,000 spikes per month for each component, see Tables 1, 2, 5) the manual filtering procedure becomes extremely laborious. Moreover, they should not be confused with geomagnetic pulsations or other geophysical events (Fig. 5), which should not be removed. The complete statistical information on the events detected by eye, including

Table 3. Statistics on the events recognized by the algorithm $SPm = SPm(\pi^*)$ from 1/07/2009 to 20/07/2009.

Channel	Spikes recognized by eye	Events recognized by the algorithm	Missed spikes	Extra events	Probability of an error of the 1st kind	Probability of an error of the 2nd kind	Quality criterion $K_{0.8}$
X	1119	1168	53	102	0.047	0.087	0.055
Y	1122	1224	39	141	0.035	0.115	0.051
Z	996	1007	170	181	0.171	0.180	0.172
F	1135	1146	134	145	0.118	0.127	0.120

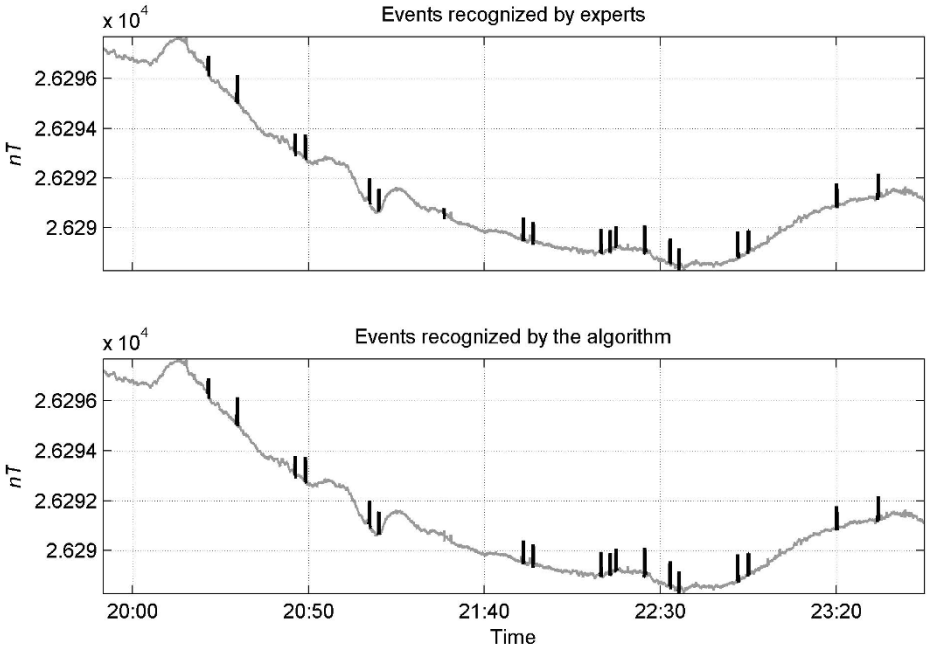

Fig. 6. Comparison between algorithm (bottom) and manual (top) recognition results (X component, 1 July 2009). In both cases recognized spikes are marked with black.

estimation of spike amplitudes and durations, is given in Tables 1 and 2.

The first part of the testing dataset, from 1 to 20 July 2009, was used for the training of the algorithm. As can be seen in Table 1 the mean spike amplitude vary from one channel to the next, and therefore we performed algorithm learning for each channel X, Y, Z, F separately. As a result, we were able to obtain the optimal free parameter values of the algorithm for each channel independently. In order to select optimal values of free parameters, we implemented a brute-force search, i.e., we systematically tried a large number of values (Knuth, 1968). First, each 1-day 1-channel data series was processed by the algorithm using the following set of free parameter values:

$$\Pi = \left\{ \begin{array}{l} \nu = 0.4, 0.5, 0.6, 0.7; \\ \rho_1 = 0.45, 0.5, 0.55, 0.6, 0.65; \\ \rho_2 = 0.2, 0.25, 0.3, 0.35, 0.4 \end{array} \right\}.$$

These values were pre-selected based upon the known behavior of the fuzzy comparison function and some preliminary tests. In total, $|\Pi| = 100$ combinations of free parameters were tested. To assess recognition quality we introduce the following function to be minimized:

$$K_\lambda(SPs(\pi)) = \lambda P_1(SPs(\pi)) + (1-\lambda)P_2(SPs(\pi)),$$

where $SPs(\pi)$ is a result of the algorithm operation with some combination of free parameter values π expressed in a set of intervals on the time axis, which define recognized events; P_1 is the probability of the first kind error (target miss) defined as $\frac{N_{\text{missed}}}{N_{\text{eye}}}$ (where N is the number of spikes); P_2 is the probability of the second kind error (false alarm) defined as $\frac{N_{\text{false}}}{N_{\text{algorithm}}}$; $0 \le \lambda \le 1$ (Bogoutdinov *et al.*, 2010). In the criterion K_λ we put $\lambda = 0.8$, thus expressing a higher degree of importance of not missing spikes versus avoiding false alarms. The value of the parameter λ was obtained by testing the algorithm for $\lambda = 0.1, 0.2, \ldots, 0.9$ on an arbitrary set of free parameters and selecting the value for which the best recognition was achieved.

One should note that the range of free parameter values given above is quite wide. In order to better identify free parameter values, we took a small neighborhood around the already found optimal solution. It entailed examination of additional 125 combinations of free parameters. Following the same line for assessing the recognition quality as on the first stage of learning, we obtained the optimal free parameter values for each channel. In Bogoutdinov *et al.* (2010), it was shown that different optimal combinations of the free parameters were found for different observatories recording one-minute data. It is expected that a similar situation will arise in the case of other observatories recording one-

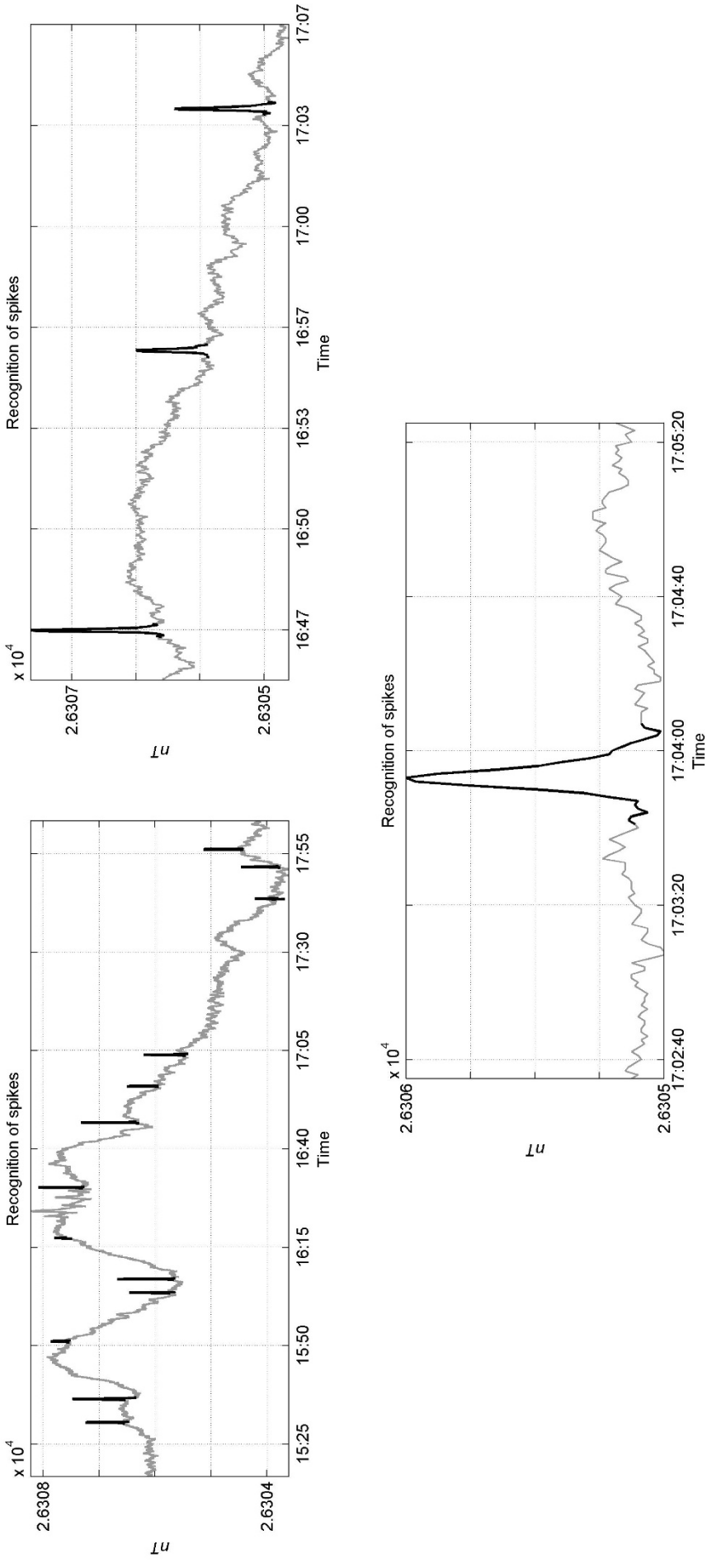

Fig. 7. Examples of spike recognition by the algorithm *SPs* (*X* component, 1 July 2009). Recognized spikes are marked with black.

Table 4. Statistics on the events recognized by the algorithm $SPm = SPm(\pi^*)$ from 21/07/2009 to 31/07/2009.

Channel	Spikes recognized by eye	Events recognized by the algorithm	Missed spikes	Extra events	Probability of an error of the 1st kind	Probability of an error of the 2nd kind	Quality criterion $K_{0.8}$
X	853	854	50	51	0.059	0.060	0.059
Y	844	884	36	76	0.043	0.086	0.051
Z	774	731	108	65	0.140	0.089	0.129
F	846	789	124	67	0.147	0.085	0.134

Table 5. Results of application of the algorithms $SPs(\pi_X^*)$, $SPs(\pi_Y^*)$, $SPs(\pi_Z^*)$ and $SPs(\pi_F^*)$ to the records obtained from 1 to 31 August 2009 and their assessment by experts.

Channel	Spikes recognized by eye	Events recognized by the algorithm	Missed spikes	Extra events	Probability of an error of the 1st kind	Probability of an error of the 2nd kind	Quality criterion $K_{0.8}$
X	2122	2057	79	14	0.0372	0.0068	0.031
Y	2143	2150	23	30	0.0107	0.0140	0.011
Z	1786	1780	104	98	0.0582	0.0551	0.058
F	1963	1996	39	72	0.0199	0.0361	0.023

second data.

Once the free parameters were fixed, we first tested the algorithm by applying it to the time interval from 21 to 31 July 2009 and comparing with the results of manual data cleaning. By separating the dataset in two parts, we thus made sure that the testing was performed on an independent dataset. Next, we applied the algorithm to the time interval from 1 to 31 August 2009 and then performed recognition of spikes by eye in order to check the results.

4. Results

4.1 Results of the learning phase

The following optimal free parameter values were found to give the best results for the overall criterion of recognition $K_{0.8}$ for each channel:

$$\pi_X^* = (\nu = 0.46, \rho_1 = 0.45, \rho_2 = 0.44);$$
$$\pi_Y^* = (\nu = 0.50, \rho_1 = 0.41, \rho_2 = 0.44);$$
$$\pi_Z^* = (\nu = 0.56, \rho_1 = 0.43, \rho_2 = 0.44);$$
$$\pi_F^* = (\nu = 0.50, \rho_1 = 0.43, \rho_2 = 0.44).$$

The overall numbers of target misses and false alarms as well as the values of the recognition criterion for each component are provided in Table 3. The best results of the algorithm learning were achieved in the case of the horizontal components X and Y, where the error probabilities varied between 3.5% and 11.5%. Less good results were obtained in the case of the vertical component Z, where the error probabilities of the first and the second kinds were 17.1% and 18.0% correspondingly. This difference is attributed to the smaller average amplitude of the spikes on the Z component during the learning phase time interval, which made them more difficult to detect.

Some screenshots illustrating application results of the algorithm $SPs = SPs(\pi_X^*)$ are given in Figs. 6 and 7.

4.2 Results of the testing phase

The results of the testing phase are provided in Table 4. Comparison of recognition results obtained on data for 1–20 July (learning material) and 21–31 July (testing material) shows that the recognition quality is about the same. Formally it is confirmed by very close values of the calculated quality criterion (Tables 3, 4). It can be concluded that the overall recognition performance achieved during the learning phase could be reproduced during the testing phase.

4.3 Results of the blind test

The blind test involved data recorded from 1 to 31 August 2009 with no *a priori* expert opinion. The results of the recognition by the algorithm $SPs = SPs(\pi^*)$ were subsequently evaluated by eye. The overall recognition statistics for the whole set of data are provided in Table 5.

The probability of missed spikes for the X component is 3.72%, that of false alarms is 0.68%, to be compared with 4.7% of missed spikes and 8.7% of false alarms for the 1/07–20/07 time interval (Table 3) and 5.9% of missed spikes and 6.0% of false alarms for the 21/07–31/07 time interval (Table 4). In the case of the other components Y, Z and the total intensity F the blind test also demonstrated higher efficiency of the algorithm application comparing to results of learning and testing phases, which is well reflected in the corresponding values of $K_{0.8}$ quality criterion (Tables 3–5).

The difference in algorithm recognition quality $K_{0.8}$ obtained for records for August and July 2009 is likely due to the fact that it was easier to carry out manual data processing by eye having at the disposal the results of the algorithm recognition (August data), rather than to analyze raw magnetograms "from scratch" (July data). Thus for July data the quality of manual recognition of spikes turned to be worse. This shows that the algorithm significantly helped the recognition by eye. It also provides some estimate of the amount of errors made when relying on manual spike detection.

Missed spikes and extra events recognized by the algorithm in August data were separately examined and the following conclusions were made: usually extra events represent either geomagnetic pulsations or other natural geomagnetic signals occurring in a narrow frequency band, whereas missed spikes in some cases represent long anomalous in-

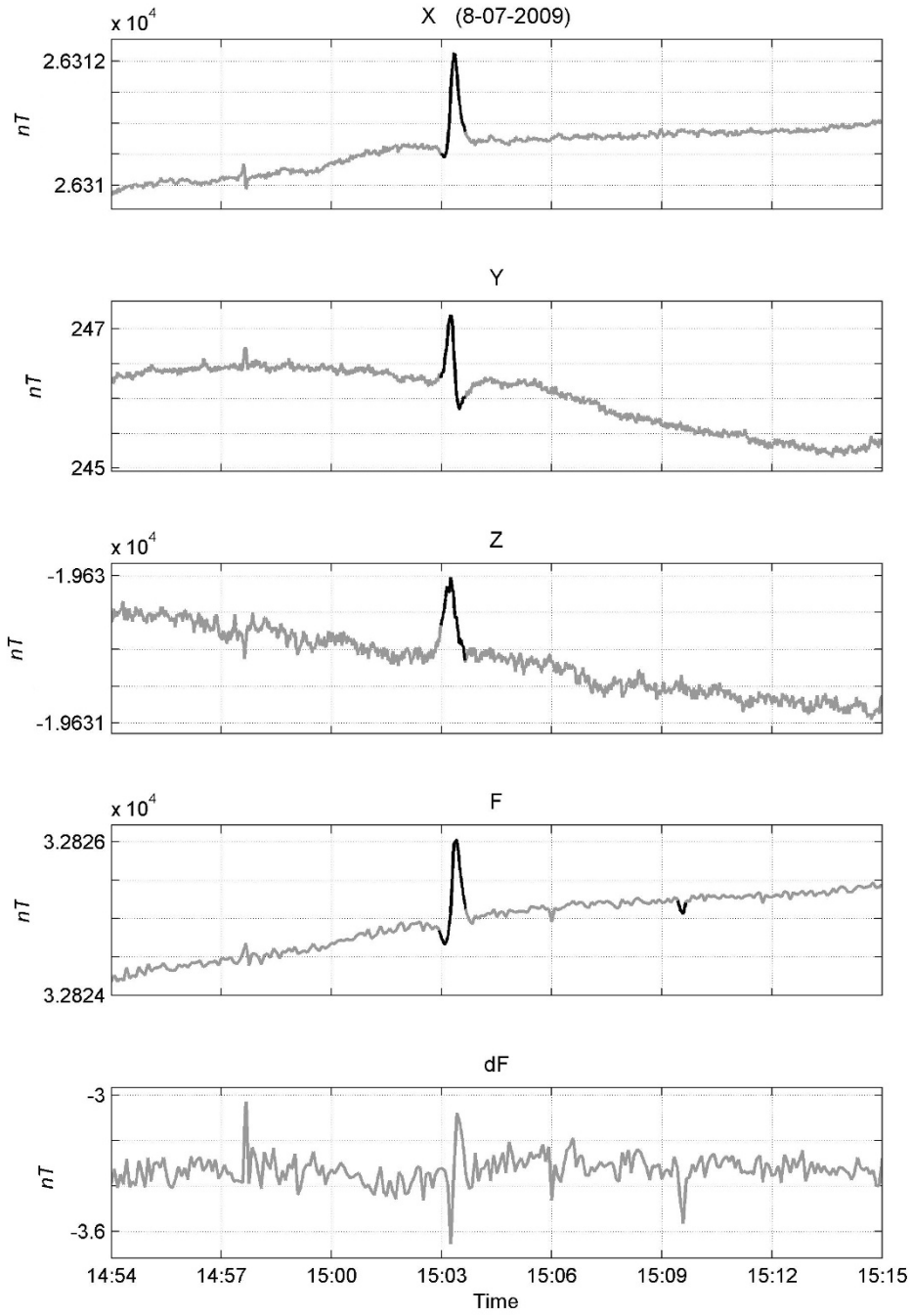

Fig. 8. Example of "false spike" seen on dF record (bottom) on the left. Spikes recognized by eye on initial records X, Y, Z and F are marked on the corresponding records with black. The "false spike" seen on dF record could be representative of low amplitude spikes on X, Y, Z and F records and therefore less visible in the background noise of the X, Y, Z and F recordings.

tervals not caused by trucks or airplanes.

The results of the blind test confirm that the learned algorithm is able to detect most of the spikes, and shows that there is some variability from one day/week/month to the next.

5. Discussion

In the present paper we introduced the algorithm *SPs*, able to automatically recognize spikes caused by artificial disturbances in magnetic observatory data sampled every second. We applied this algorithm to the recently installed observatory in Easter Island, where nearby trucks and planes cause several tens of such spikes every day. We showed that, after a 20-day learning phase in July 2009, the algorithm is able to recognize more than 94% of the spikes on the three components and the intensity recordings in August 2009, while the percentage of false alarms is less than 6%. At all the stages the algorithm showed worse results in processing vertical component Z.

A detailed examination of the false alarms reveals that most of them are due to geomagnetic pulsations. It is indeed very difficult sometime, even for a trained data expert, to distinguish a pulsation from an artificial spike. The occurrence of a pulsation can generally be inferred from

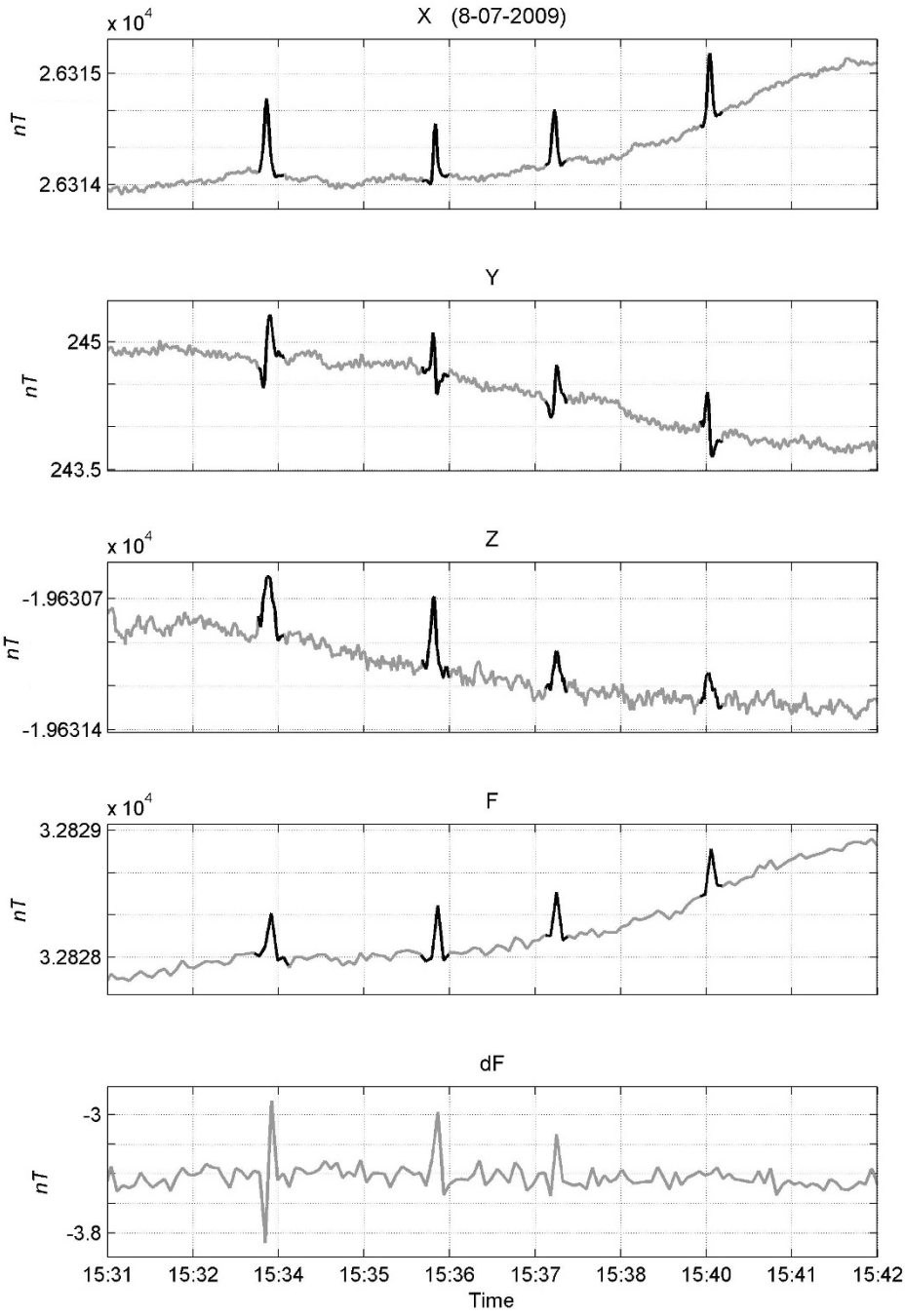

Fig. 9. Example of a spike absence on dF record (bottom) on the right. Spikes recognized by eye on initial records X, Y, Z and F are marked on the corresponding records with black.

the simultaneous occurrence of a pulsation-like signal at a nearby observatory. This functionality is not included in the present version of the algorithm. In some rare cases, false alarms are due to the temporary increase of the background noise, whose origin is unknown.

A standard method to detect spikes in magnetic observatories consists in taking the difference $dF = F_s - F_v$ between the field modulus $F_s = F$ directly measured by the scalar magnetometer and that F_v calculated from the three components measured by the vector magnetometer. Normally, dF should vary by a up to a few tenths of nT around a constant non-zero value due to the differences in transfer functions and locations of the instruments. Instrumental spikes and other anomalies generally lead to a larger than normal value of dF, which can easily be detected. Typical IPM disturbances caused by nearby trucks and planes do also cause an increase of the dF absolute value, due to the distance between the two magnetometers (about two meters) and their different transfer functions. However, in some cases, the resulting dF spike is not easily distinguishable from the instrumental noise, as can be seen in the example shown in Fig. 8. On the contrary, quite often dF record does not reflect spikes, which are present in initial geomagnetic records. The corresponding example is given in Fig. 9. It should be noted that the both examples lie within one hour period of one day.

Another disadvantage of dF method is that it needs presence of both vector data on the three components and scalar data on total field intensity and consequently correct operation of the both devices is required. The method becomes invalid if one of the devices doesn't work properly or registration of one of the three vector components is failed. On the contrary, data filtration using the *SPs* algorithm can be applied to any particular record regardless of the presence of other records. It makes the algorithm applicable not only at magnetic observatories but also at magnetic stations where only variational data registration is carried out.

We plan to carry out further studies on seasonal and activity level dependence of the recognition results. The described algorithm is currently being implemented in the operation of the Russian-Ukrainian geomagnetic data center hosted by the Geophysical Center of the Russian Academy of Sciences. The development of a web application based upon the *SPs* algorithm is also being considered, in order to make it available to the wider magnetic observatory community.

Acknowledgments. We thank Alan W. P. Thomson and Hans-Joachim Linthe for constructive reviews. The research has been carried out in the framework of collaboration program between Institut de Physique du Globe de Paris (IPGP), Moscow Institute of Physics of the Earth of Russian Academy of Sciences (IPE RAS) and Geophysical Center of RAS (GC RAS). The development of the algorithm *SPs* has been carried out in the framework of the project number 12-05-90428 supported by Russian Foundation for Basic Research. The Easter Island (IPM) magnetic observatory is jointly operated by Dirección Meteorológica de Chile (DMC) and IPGP. We thank INTERMAGNET for promoting high standards of magnetic observatory practice (www.intermagnet.org). This is IPGP contribution number 3288.

References

Agayan, S. M., S. R. Bogoutdinov, A. D. Gvishiani, E. M. Graeva, J. Zlotnicki, and M. V. Rodkin, Study of signal morphology basing on fuzzy logic algorithms, *Geophys. Res. Proc. Moscow, IPE RAS*, **1**, 143–155, 2005 (in Russian).

Bogoutdinov, S. R., A. D. Gvishiani, S. M. Agayan, A. A. Solovyev, and E. Kihn, Recognition of disturbances with specified morphology in time series. part 1: spikes on magnetograms of the worldwide INTERMAGNET network, *Izv. Phys. Solid Earth*, **46**(11), 1004–1016, 2010.

Chulliat, A., X. Lalanne, L. R. Gaya-Piqué, F. Truong, and J. Savary, The new Easter Island magnetic observatory, in *Proceedings of the XIIIth IAGA Workshop on Geomagnetic Observatory Instruments, Data Acquisition and Processing*, edited by J. J. Love, 271 pp., U.S. Geological Survey Open-File Report 2009-1226, 2009a.

Chulliat, A., J. Savary, K. Telali, and X. Lalanne, Acquisition of 1-second data in IPGP magnetic observatories, in *Proceedings of the XIIIth IAGA Workshop on Geomagnetic Observatory Instruments, Data Acquisition and Processing*, edited by J. J. Love, 271 pp., U.S. Geological Survey Open-File Report 2009-1226, 2009b.

Draper, N. R. and H. Smith, *Applied Regression Analysis*, 407 pp., Wiley, New York, 1966.

Gvishiani, A. D., S. M. Agayan, Sh. R. Bogoutdinov, J. Zlotnicki, and J. Bonnin, Mathematical methods of geoinformatics. III. Fuzzy comparisons and recognition of anomalies in time series, *Cybern. Syst. Anal.*, **44**(3), 309–323, 2008a.

Gvishiani, A. D., S. M. Agayan, and Sh. R. Bogoutdinov, Fuzzy recognition of anomalies in time series, *Dokl. Earth Sci.*, **421**(5), 838–842, 2008b.

Gvishiani, A. D., S. M. Agayan, S. R. Bogoutdinov, and A. A. Soloviev, Discrete mathematical analysis and geological and geophysical applications, *Vestnik KRAUNZ. Earth Sciences, 2*, **16**, 109–125, 2010 (in Russian).

Knuth, D., *The Art of Computer Programming. Volume 3: Sorting and Searching*, 800 pp., Addison-Wesley, USA, 1968.

Love, J. J., Magnetic monitoring of Earth and space, *Phys. Today*, **61**, 31–37, 2008.

Marshall, R. A., E. A. Smith, M. J. Francis, C. L. Waters, and M. D. Sciffer, A preliminary risk assessment of the Australian region power network to space weather, *Space Weather*, **9**, S10004, doi:10.1029/2011SW000685, 2011.

Matzka, J., A. Chulliat, M. Mandea, C. Finlay, and E. Qamili, Geomagnetic observations for main field studies: from ground to space, *Space Sci. Rev.*, **155**, 29–64, doi:10.1007/s11214-010-9693-4, 2010.

Reay, S. J., W. Allen, O. Baillie, J. Bowe, E. Clarke, V. Lesur, and S. Macmillan, Space weather effects on drilling accuracy in the North Sea, *Ann. Geophys.*, **23**, 3081–3088, doi:10.5194/angeo-23-3081-2005, 2005.

Samson, J. C., Geomagnetic pulsations and plasma waves in the Earth's magnetosphere, in *Geomagnetism. Vol. 4*, edited by J. A. Jacobs, 481–592, 825 pp., Academic Press, London, 1991.

Soloviev, A. A., Sh. R. Bogoutdinov, S. M. Agayan, A. D. Gvishiani, and E. Kihn, Detection of hardware failures at INTERMAGNET observatories: Application of artificial intelligence techniques to geomagnetic records study, *Russ. J. Earth Sci.*, **11**, ES2006, doi:10.2205/2009ES000387, 2009.

Soloviev, A. A., S. M. Agayan, A. D. Gvishiani, S. R. Bogoutdinov, and A. Chulliat, Recognition of disturbances with specified morphology in time series. Part 2: Spikes on 1-second magnetograms, *Izv. Phys. Solid Earth*, 2012 (accepted).

St-Louis, B., *INTERMAGNET Technical Reference Manual, Version 4.4*, 86 pp., 2008.

Worthington, E. W., E. A. Sauter, and J. J. Love, Analysis of USGS one-second data, in *Proceedings of the XIIIth IAGA Workshop on Geomagnetic Observatory Instruments, Data Acquisition and Processing*, edited by J. J. Love, 271 pp., U.S. Geological Survey Open-File Report 2009-1226, 2009.

Zadeh, L. A., Fuzzy sets, *Inf. Control.*, **8**, 338–353, 1965.

A. Soloviev (e-mail: a.soloviev@gcras.ru), A. Chulliat, S. Bogoutdinov, A. Gvishiani, S. Agayan, A. Peltier, and B. Heumez